

# $\Lambda_c^+$ production in Au+Au collisions at 200 GeV at sPHENIX

Yuanjing Ji ([jiyj@mail.ustc.edu.cn](mailto:jiyj@mail.ustc.edu.cn))<sup>1,2</sup>, Xiaolong Chen<sup>1</sup>, and Dong Xin<sup>2</sup>

<sup>1</sup>*University of Science and Technology of China, Hefei 230026, China*

<sup>2</sup>*Lawrence Berkeley National Laboratory, Berkeley, California 94720, USA*

(Dated: 2019-04-09)

## Contents

<b>1</b>	<b>Introduction</b>	<b>1</b>
<b>2</b>	<b>Simulation approach</b>	<b>1</b>
2.1	sPHENIX detector performance . . . . .	2
2.2	Signal . . . . .	4
2.3	Combinatorial background . . . . .	5
2.4	PID scenario . . . . .	7
2.5	$\Lambda_c$ reconstruction . . . . .	7
<b>3</b>	<b>Results and discussion</b>	<b>8</b>
<b>4</b>	<b>Summary</b>	<b>10</b>

## 1 Introduction

$\Lambda_c$  provides a unique opportunity to understand charm quark hadronization mechanism in QGP. Both STAR and ALICE experiment have observed strong enhancement of  $\Lambda_c^+/D^0$  ratio with respect to PYTHIA 8 calculation [6, 7]. An enhancement in baryon-to-meson ratio is expected if the deconfined charm quarks hadronized via coalescence mechanism. But different coalescence models still have large difference when it goes to the low  $p_T$ . An enhancement in  $\Lambda_c^+/D^0$  ratio suggests that  $\Lambda_c$  baryons can have sizable contribution to the total charm cross section. Furthermore, the current precision is largely limited by  $\Lambda_c$  measurement, particularly at low  $p_T$  ( $p_T \lesssim 3$  GeV). In this simulation, we estimate the performance of  $\Lambda_c$  production measurement in Au+Au collisions at  $\sqrt{s_{NN}} = 200$  GeV utilizing sPHENIX with MVTX detector.

## 2 Simulation approach

As it will be quite time costly to get enough statistics if running the full Hijing simulation and passing all of the final particles into the Geant4 simulation package, so this simulation is based on a hybrid method, similar as  $D^0$  and  $B^+$  simulation [1]. We first embed single particles ( $\pi^\pm, p/\bar{p}, K^\pm$ ) into the full Geant4 simulation of the detector, plus with tracking, to extract single track performance, such as  $DCA_{XY}$  and  $DCA_Z$  distribution, momentum resolution and tracking efficiency (TPC+INTT+MVTX). Then we take the single track performance as the input to run the fast simulation. This method have already validated in the  $D^0$  measurement at the STAR experiment [5], when they apply a data-driven simulation to calculate the reconstruction efficiency of  $D^0$ . The validation procedure is also mentioned in  $D^0$  and  $B^+$  simulation note [1].

The overview of the simulation flow is summarized in Fig. 1. The basic procedure is:

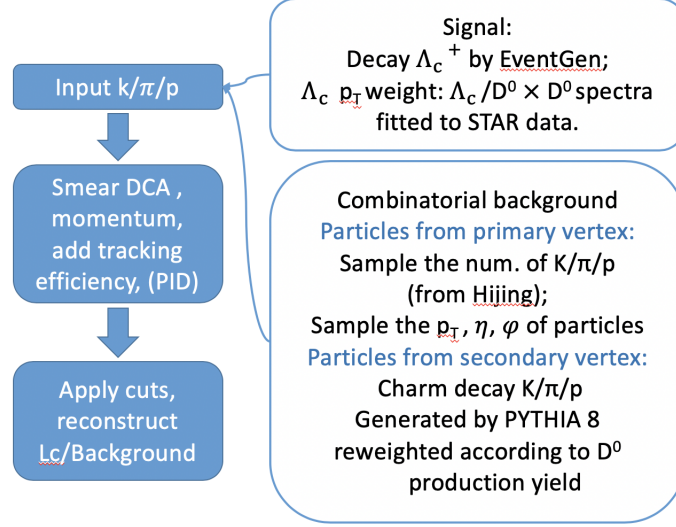


Figure 1: caption

1. Sample the primary vertex position in Z-direction ( $V_z$ ) according to the data or projected distribution. Fix to 0 in this simulation.
2. Generate the final state particles: K,  $\pi$  and p. The distribution, four momentum and origin position of the particles will be determined in this step. Details will be discussed in the following signal and background section.
3. Smear the  $K/\pi/p$  momentum according to the momentum resolution. Smear  $K/\pi/p$  origin position according to  $DCA_{XY}$  vs  $DCA_Z$  2D distribution.
4. Apply tracking efficiency, TOF matching efficiency (if needed) and PID cut (if needed). We consider 4 PID condition, which will be discussed later.
5. Reconstruct the secondary vertex of  $\Lambda_c$  candidate as in real analysis and apply topological cuts. The  $\Lambda_c$  is reconstructed through  $\Lambda_c^+ \rightarrow p\pi^+K^-$ .

## 2.1 sPHENIX detector performance

We follow the same method as  $D^0$  and  $B^+$  simulation to study sPHENIX detector performance[1]. 100  $K/\pi/p$  are embedded into the full Geant4 simulation of sPHENIX. The samples used are the same as used in the previous  $D^0$  and  $B^+$  simulation study. Fig. 2 is the tracking efficiency as a function of  $p_T$  including TPC tracking efficiency and MVTX matching efficiency. MVTX matching requires the track has at least two layers MAPS hits. The distribution is fitted with the following formula:

$$Eff = N \times e^{-(p_T/a)^b} \quad (1)$$

The DCA distribution of the  $K/\pi/p$  is extracted in 2 dimension considering the  $DCA_{xy}$  vs  $DCA_z$  correlation in the barrel-like detector systems (TPC, MVTX etc). Fig. 4 is the  $DCA_{xy}$  vs  $DCA_z$  at  $0.8 < p_T < 0.9$  GeV. DCA is the distance of closet approach between particles tracks and event primary tracks. The particles embedded in the detectors are primary particles, but as the detectors' performance in spacial resolution should be the same no matter this tracks are from secondary decay or primary tracks. Thus we are able to use this DCA distribution to smear the primary tracks' global DCA and the secondary tracks' DCA at secondary vertex. We project the DCA under each  $p_T$  bins and use gaussian function to fit it to extract the resolution at this  $p_T$  bin, so that finally we could get the DCA resolution as function as  $p_T$ , shown in Fig. 3 (right). The full DCA distributions are used when smearing particle positions in our

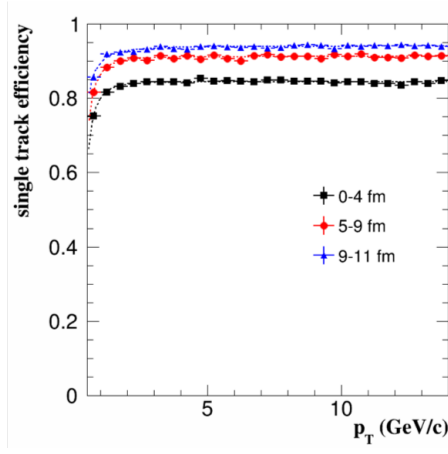


Figure 2: Tracking efficiency used in this simulation

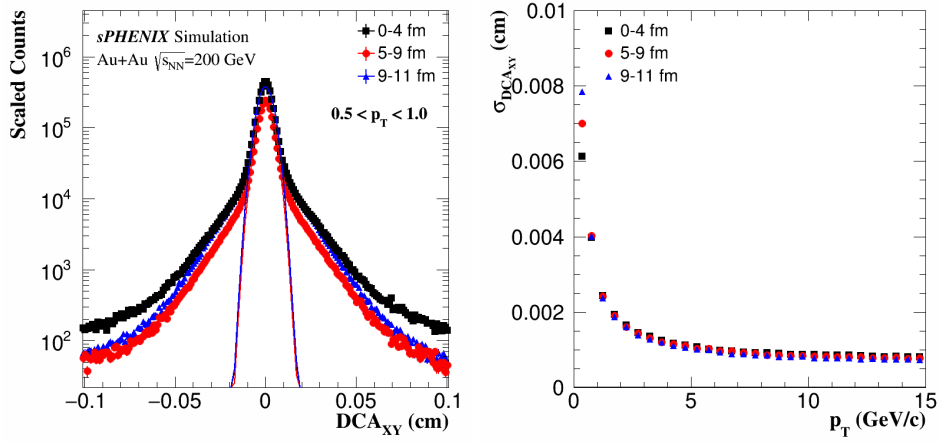


Figure 3:  $DCA_{XY}$  resolution of K/p/ $\pi$

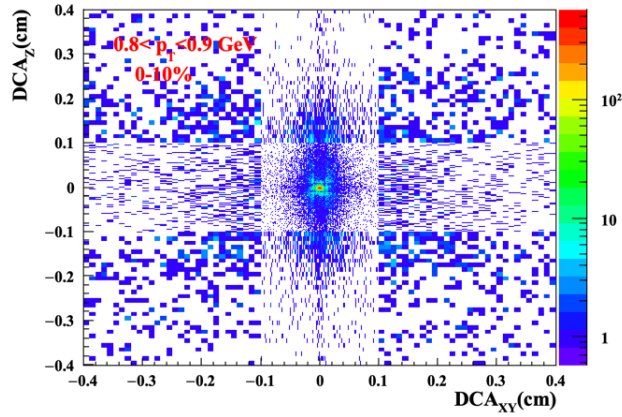


Figure 4: K/p/ $\pi$   $DCA_Z$  VS  $DCA_{XY}$  2D distribution

fast simulation calculation. Fig. 3 (left) is an example of  $K/\pi/p$   $dp_T/p_T^{true}$  distribution at  $3.1 < p_T < 3.3 \text{ GeV}$ . Here,  $dp_T = p_T^{res} - p_T^{true}$ ,  $p_T^{res}$  is the reconstructed momentum and  $p_T^{true}$  is MC  $p_T$ . We use gaussian function to fit  $dp_T/p_T^{true}$  projection under each  $p_T$  bin to extract the momentum resolution and Fig. 5 (right) is  $\sigma p_T/p_T^{true}$  as function as  $p_T$ . The fitting function for the right plot of Fig. 5 is:

$$\frac{\sigma p_T}{p_T} = \sqrt{\left(\frac{a}{\sqrt{p_T}}\right)^2 + (b \cdot p_T)^2 + c^2} \quad (2)$$

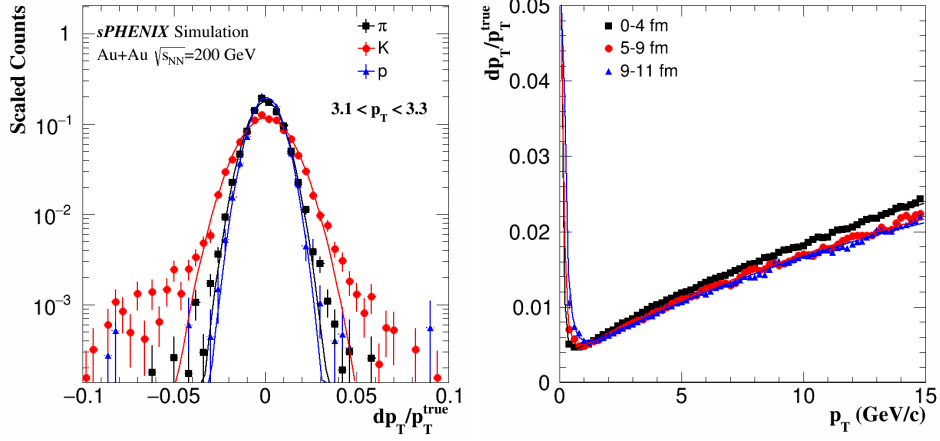


Figure 5: Momentum resolution of K/p/π in this simulation

## 2.2 Signal

We use the EvtGen generator to generate and decay  $\Lambda_c$ .  $\Lambda_c$  are forced to decay to proton, kaon and pion ( $\Lambda_c^+ \rightarrow p\pi^+K^-$ ). The decay includes three resonant channels as well as the non-resonant channel according to the PDG measurement. We sample uniform rapidity distribution from -1 to 1, and flat  $\phi$  distribution from 0 to  $2\pi$ . For the  $p_T$  distribution, we first sample the flat  $p_T$  distribution from 0 to 15 GeV, then set the  $p_T$  weight according to the  $\Lambda_c$   $p_T$  spectra. The branch ratio (6.23%) will be applied when calculating the signal yield and the signal significance. Presently although models based on calenscence mechanism all predict an enhancement at middle  $p_T$ , different calenscence models still have large difference at  $p_T < 3\text{GeV}$ . Furthermore, the experiment measurements of  $\Lambda_c$  spectra at 200 GeV is limited with only 3 points (10-80%). To give a better estimation of  $\Lambda_c$  spectra, we combine model calaculations with experiment data. The  $\Lambda_c p_T$  spectra shape is estimated by  $\Lambda_c/D^0 \times D^0$  spectra.  $\Lambda_c/D^0$  curves are taken using the average calculation from the following models: Ko: di-quark, Ko: three-quark, Greco, Tshingua. The preliemary result of  $\Lambda_c/D^0$  ratio in Au+Au 200 GeV measured by STAR and comparason with models is shown in the Fig. 6. The  $D^0$  spectra is gotten from the STAR measurement (at 10-80%), shown in Fig. 6 [5]. Then we use these spectra shapes to fit the  $\Lambda_c$  spectra from the STAR measurement. The final  $\Lambda_c$  spectra at 10-80% is the mean of these fitting results. To scale the  $\Lambda_c$  spectra to a certain centrality, we consider two sources.

Firstly, the integral yield ( $3 < p_T < 6\text{GeV}$ ) of  $\Lambda_c/D^0$  ratio vs centrality. We use quadratic function to fit the three points from STAR measurement shown in Fig. 7. Then the first weight is:

$$w_1 = \frac{\Lambda_c/D^0(N_{\text{participants of certain centrality}})}{\Lambda_c/D^0(N_{\text{participants of 10-80\%}})} \quad (3)$$

0-10%	10-20%	20-40%	40-60%	60-80%
1.37	1.3	1.12	0.89	0.74

Table 1: Weight from the centrality dependence of  $\Lambda_c/D^0$  ( $w_1$ )

Secondly, the centrality dependence of  $D^0$  spectra. The reweight is based on the integral yield of  $D^0$  at  $2 < p_T < 10\text{GeV}$ :

$$w_2 = \frac{\text{Integral yield of } D^0 \text{ at } 2 < p_T < 10 \text{ GeV at certain centrality}}{\text{Integral yield of } D^0 \text{ at } 2 < p_T < 10\text{GeV at 10-80\%}} \quad (4)$$

The corresponding weights for the centrality bin used in our simulation is listed in Table 1 and Table 2. In the real data analysis, we usually combine  $\Lambda_c^+$  and  $\Lambda_c^-$  to increase statistics, so totally  $weight = 2w_1w_2 \times branchratio$ .

0-10%	10-20%	20-40%	40-60%	60-80%
4.12	2.74	1.51	0.51	0.11

Table 2: Weight from the centrality dependence of  $D^0$  spectra ( $w_2$ )

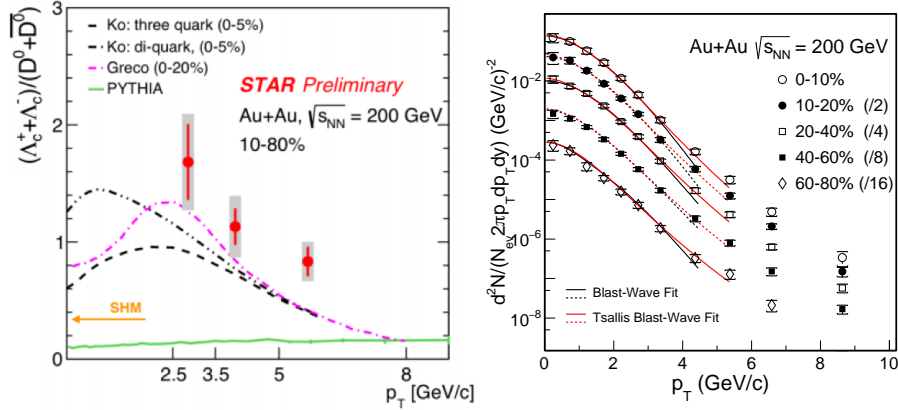
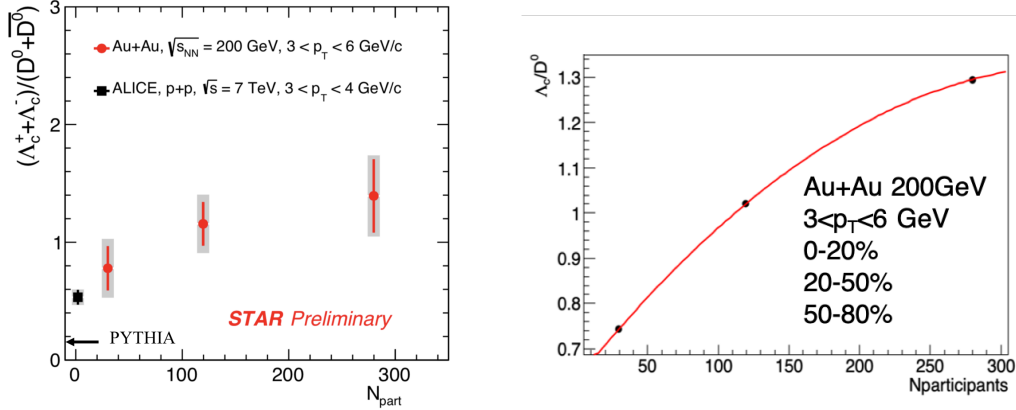


Figure 6:  $\Lambda_c/D^0$  VS  $p_T$  in Au+Au collisions at 200 GeV[6](left) and  $D^0$  spectra in Au+Au collision at 200GeV from STAR (right).



(a) Experiment results from STAR and ALICE

(b) Fitting the STAR data by quadratic function

Figure 7:  $\Lambda_c/D^0$  VS  $N_{participants}$

### 73 2.3 Combinatorial background

For the combinatorial background, which is from random combination of  $\pi/K/p$ , we consider both primary tracks and tracks from secondary vertex. For the primary tracks, the number of different particle species in a event sampled from HIJING. We sample the flat  $\eta$  distribution of  $\pi/K/p$ . The  $p_T$  is sampled according to the  $p_T$  spectra from STAR and PHENIX measurement[2, 3, 4], shown is Fig. 8. For the secondary tracks, we consider  $\pi/K/p$  from charm decay as the first order contribution. These secondary tracks are generated by PYTHIA8. We only select those final state particles from charm-decay in the p+p events generated by PYTHIA8. In the reconstruction process, if 3 daughter particles are all from charm-decay and their mother particle is the same  $\Lambda_c$  then we will discard it. To normalize p+p events from PYTHIA 8 to Au+Au collisions, we take  $D^0$  production yield as the reference. Fig. 9 is the  $D^0$  spectra in PYTHIA p+p event scaled to Au+Au collision at 60-80% centrality.

$$weight = \frac{D^0 \text{ yield } (2 < p_T < 10 \text{ GeV}) \text{ in PYTHIA 8}}{D^0 \text{ yield } (2 < p_T < 10 \text{ GeV}) \text{ from STAR measurement}} \quad (5)$$

74 After generate all of the background  $\pi/p/K$  tracks. We follow out fast simulation procedure,  
75 judging whether each track can be identified or mis-identified and reconstructing the  $\Lambda_c$ . To

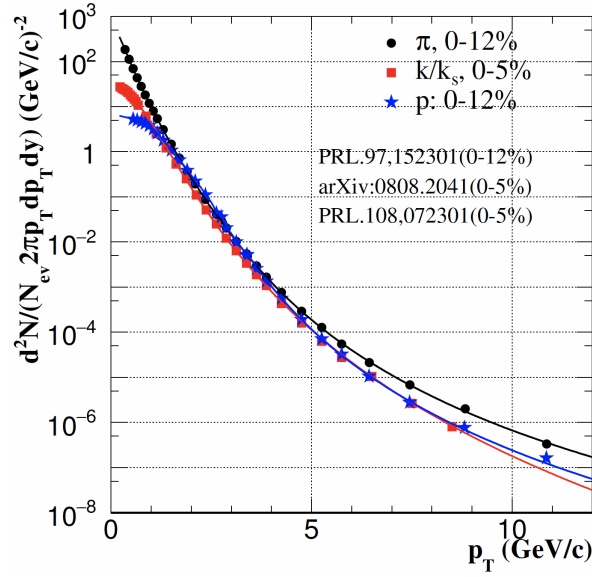


Figure 8: K/p/π spectra in Au+Au 200GeV[2, 3, 4]

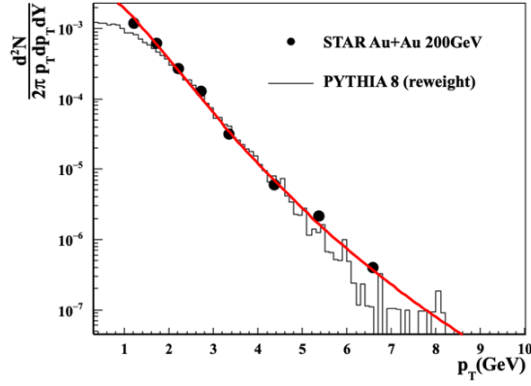


Figure 9:  $D^0$  spectra in p+p from PYHITA (scaled) and in Au+Au collision (60-80%) from STAR.

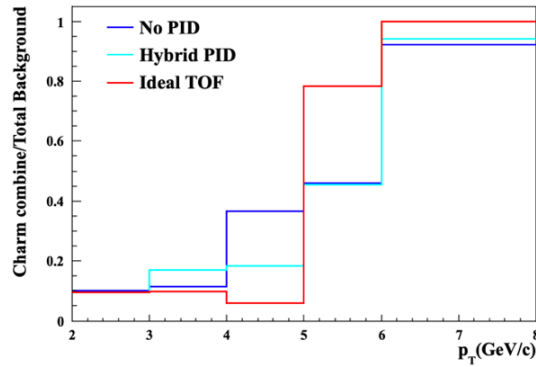


Figure 10: Backgrounds with at least one charm decay daughter to the total background ratio at 0-80%

76 estimate the contribution of charm decay daughters to the background, we draw the ratio of the  
 77 background  $Kp\pi$  pair candidates, who have at least one charm-decay daughter, over the total  
 78 backgrounds, shown in Fig. 10. From this plot, it can be inferred that charm decay daughters  
 79 do make large contribution to the background because they have similar topological parameter  
 80 as  $\Lambda_c$  when  $p_T$  goes high, but negligible at low  $p_T$ .

## 2.4 PID scenario

We consider 4 particle identification (PID) scenarios:

1. “No PID”: Suppose we do not have PID detector.
2. “Clean PID”: Particles can be identified at low  $p_T$  if the particle is accepted by TOF, and no PID at high  $p_T$ . TOF matching efficiency is defined by the number of tracks matched with TOF record over total TPC track number. The TOF performance is taken from STAR TOF detector, shown in Fig. 11 [5].
  - $K/\pi$  separation up to 1.6 GeV/c, protons up to 3 GeV/c;
  - The efficiency that particle can be identified by TOF, so called “TOF matching efficiency“, is around 58%.

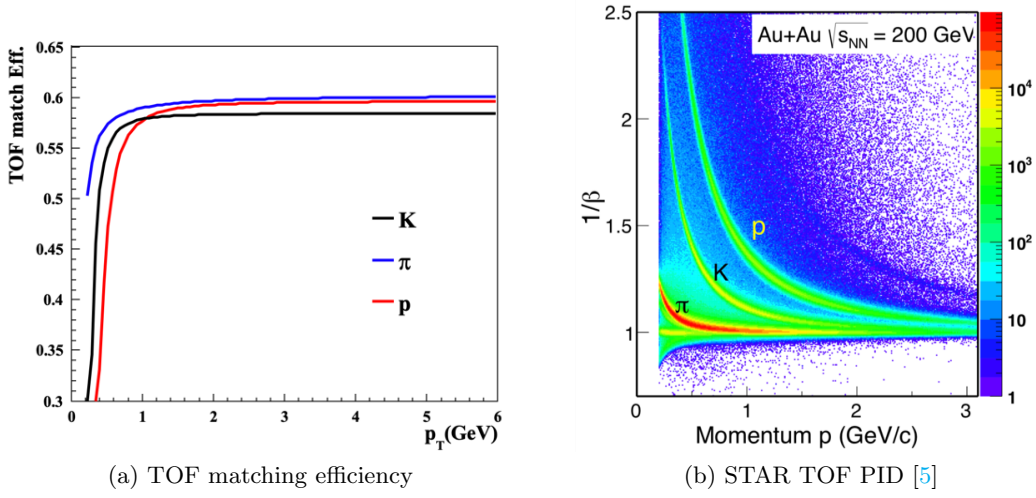


Figure 11: TOF detector performance used in this simulation

3. “Hybrid PID”: This PID is commonly used in the real data analysis to enhance statistics. We will require TOF PID if the track is matched to TOF; otherwise no PID cut.
4. “Ideal TOF PID”: This is similar as 2, but assuming 100% TOF matching efficiency.

## 2.5 $\Lambda_c$ reconstruction

$\Lambda_c$  is short life charm baryon ( $c\tau = 59.4\mu m$ ). The MVTX detector in sPHENIX is a dedicate detector perfect for secondary vertex reconstruction. We choose the following channel to reconstruct  $\Lambda_c^+$ :

$$\begin{aligned}
 \Lambda_c^+ &\rightarrow K^- p \pi^+ & 6.23\% \\
 &p \bar{K}^* & 1.94\% \times 66.7\% \\
 &\Delta(1232)^{++} & 1.07\% \times 99.4\% \\
 &\Lambda(1520) \pi^+ & 2.2\% \times 22.5\% \\
 &non - resonant & 3.4\%
 \end{aligned}$$

The basic cut on single particles is:  $p_T > 0.6 GeV$  and  $|\eta| < 1$ . The topological variables used for reconstruction is:

1. global DCA of  $K/p/\pi$ : the distance of closet approach (DCA) from  $K/\pi/p$  track to primary vertex (PV).
2. DCA12: The minimum one of the distance of closet approach between  $K\pi$ ,  $Kp$  and  $p\pi$ .



3. decay length:  $\Lambda_c$  decay length, shown in Fig. 12.

4. DCA  $\Lambda_c$ : The distance of closet approach between  $\Lambda_c$  and primary vertex.

5. pointing angle  $\theta$ : shown in the topological structure plot Fig. 12.

As signals' pointing angle is very close to 0, so we set a fix cut on  $\cos(\theta) > 0.995$ . To choose the best cut for the other 6 variables, we seek help from TMVA package. TMVA tuning rely on a correct input of S/B ratio to return a cut where we can achieve best significance. Because S/B is quite different in different centrality and  $p_T$  bins, we divide in 3 centrality bins: 0-10%, 10-40%, 40-80%, and 3  $p_T$  bins: 2-3GeV, 3-5GeV, 5-12GeV to do the training. Besides, S/B of different PID senario also varies differently, so we have to treat these 3 PID senario seperately: "No PID", "Hybrid PID", "Ideal TOF". For the clean PID, we just use "Ideal TOF" cuts. We try 2 kinds of tuning: the rectangle cuts ("CutsSA" in TMVA method) and the BDT cuts("BDT" in TMVA method). BDT cuts shows a little improvement on significance compared with rectangle cuts. Actually, as long as we divide the centrality and  $p_T$  range instead of using 0-80% events directly, TMVA will be very helpful to choose best cuts. An example of BDT response is shown in Fig. 13.

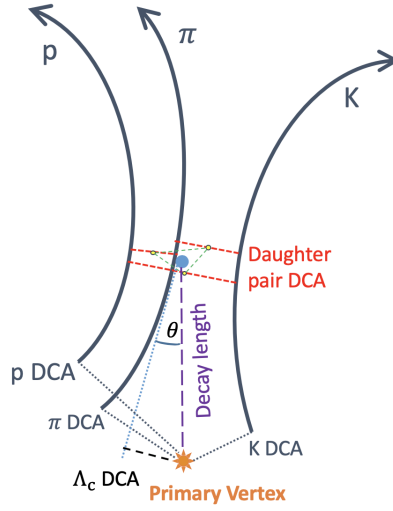


Figure 12:  $\Lambda_c$  decay topological structure

### 3 Results and discussion

To estimate the statistic error bar in the future experiment, we calculate the significance and the signal to background ratio for totally 240 billion minbias events. We generate background and signals with enough statistics for TMVA training. Then we scales the counts of signals and backgrounds within  $M \pm 3\sigma$  to 240B.  $M$  and  $\sigma$  are gotten by fitting the signals' invariant mass distribution. The significance is defined as:

$$Significance = \frac{S}{\sqrt{S+B}} \quad (6)$$

Fig. 15 an Fig. 16 is the re-sampled  $\Lambda_c$  invariant mass distribution (signal + background) under "No PID" senario at 0-80% and other centrality bins. We first fit the signal with gaussian function and then scale it to 240B events. The background is fitted by a linear function and also do the scaling. After we add the signal and background together, we use poisson distribution to resample each data point in each mass bin. The total significance of  $\Lambda_c$  we expect to achieve in sPHENIX if no PID detector is 36 in  $2 < p_T < 8GeV$  at 0-80%. The background is mainly contributed by the most central collision, which means we can have even better performance



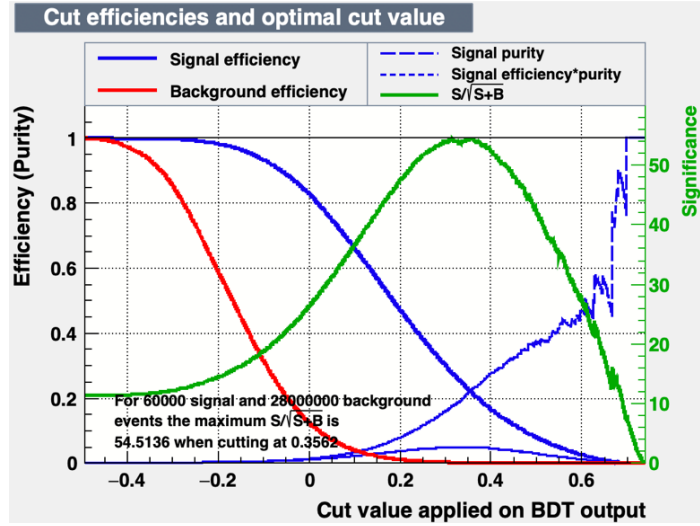


Figure 13: signal efficiency, background efficiency and significance as function as BDT evaluation value (cuts on higher BDT evaluation value results in lower signal efficiency), at 10-20%,  $3 < p_T < 5 \text{ GeV}$ .

at 10-80%. The prediction of signal significance and signal to background ratio for future  $\Lambda_c$  measurement at sPHENIX could be found at Fig. 14 for minbias events and Fig. 18 for different centrality bins. As we can see from the plots, with high statistics and better detector

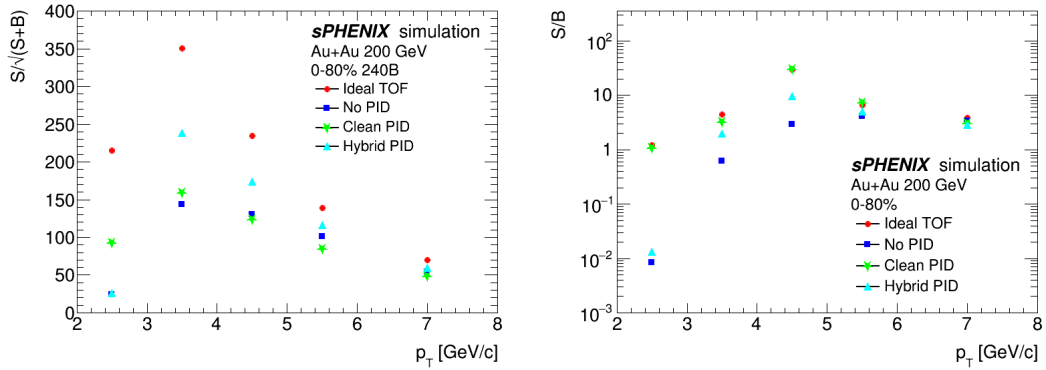


Figure 14: Significance (left) and signal to background ratio (right) of total 240 billion minbias events with 4 PID scenarios

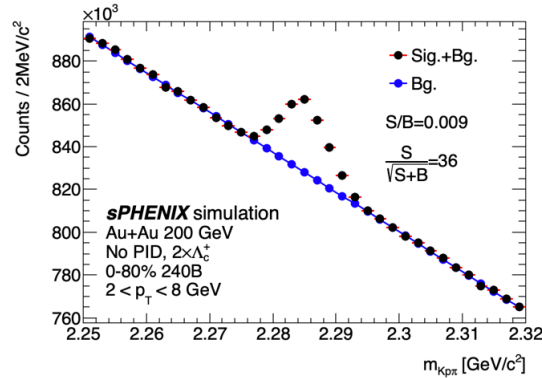


Figure 15: Resampled  $\Lambda_c$  signal at 0-80% with total 240B events

performance at sPHENIX, we can carry out more precious  $\Lambda_c$  measurement. Even at no PID condition, significance could reach  $>20$  at  $2 < p_T < 3 \text{ GeV}$  and  $> 140$  at  $3 < p_T < 4 \text{ GeV}$  at 0-

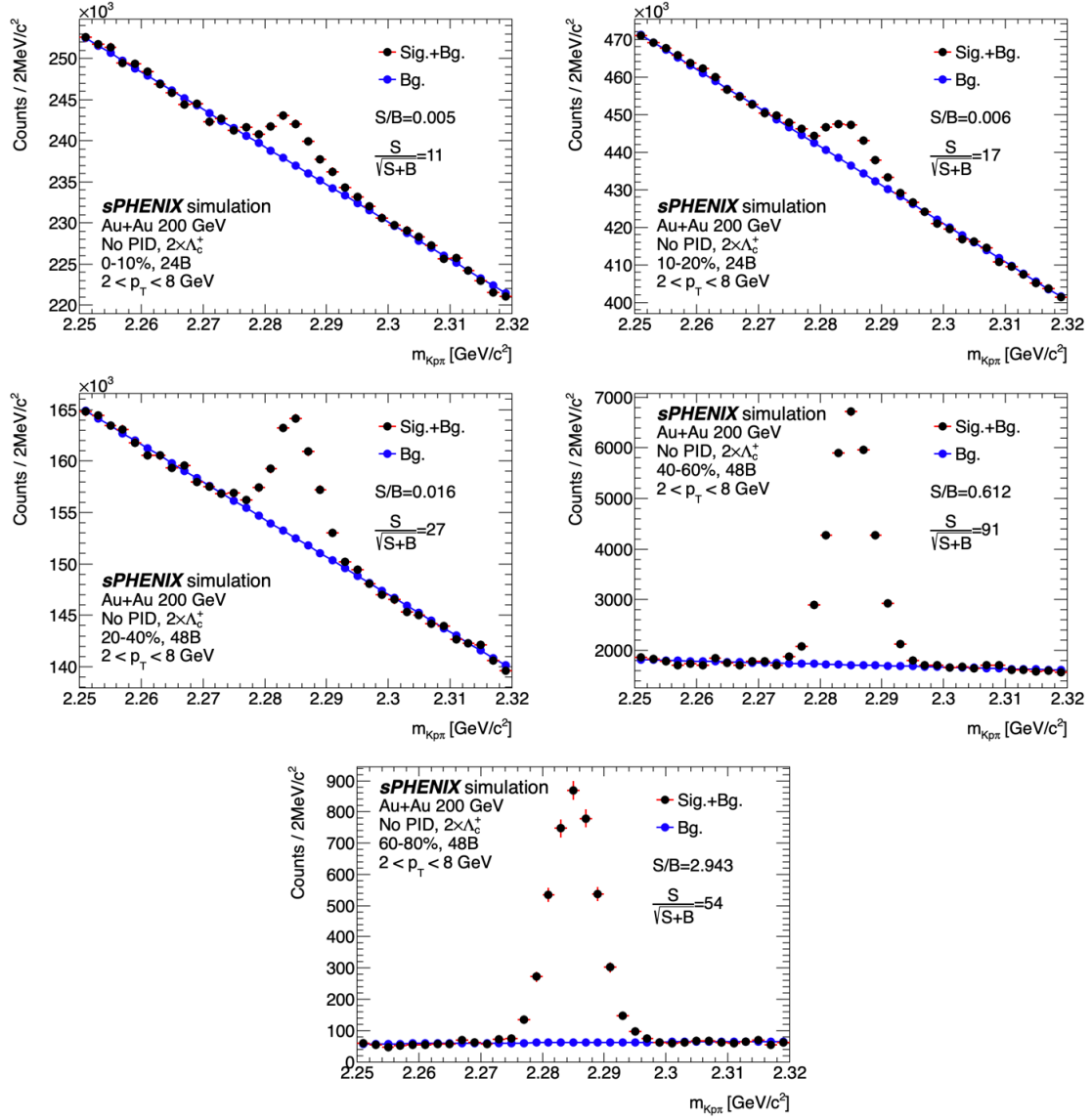


Figure 16: Resampled  $\Lambda_c$  signal at different centralities.

80%. Hopefully we can reach  $p_T < 2$  GeV for 10-80% centrality. This means we could not only constrain models but also have more precious total charm cross section measurement at Au+Au 200 GeV at low  $p_T$ . Also taking a look at the significance in different centrality bins, we could expect better centrality dependence study such as  $R_{cp}$  and  $\Lambda_c/D^0$  vs Nparticipants at sPHENIX. The significance of  $\Lambda_c$  signal is around 5 at  $2 < p_T < 3$  GeV in 0-10% under "No PID" scenario. However, the S/B ratio is only about 0.003 in this bin which may pose some sizable systematic uncertainty in the real measurement due to the background uncertainty. The S/B ratio can be improved to 0.45 if all daughter particles can be cleanly identified and the significance is 84. Fig. 17 is the physics projection plot of  $\Lambda_c/D^0$  at 0-10%. The error bar becomes larger at  $p_T = 2.5$  GeV if have no PID detector, while the error bar keeps small under ideal PID scenario. The PID detector will have a significant improvement to the  $\Lambda_c$  measurement particularly down to low  $p_T$ .

## 4 Summary

In this report,  $\Lambda_c$  measurement in Au+Au 200GeV at sPHENIX is simulated. A hybrid method is used to accelerate the computation process, which combines full Geant4 simulation of the detector and fast simulation package. With high statistics (240B MB events) and good

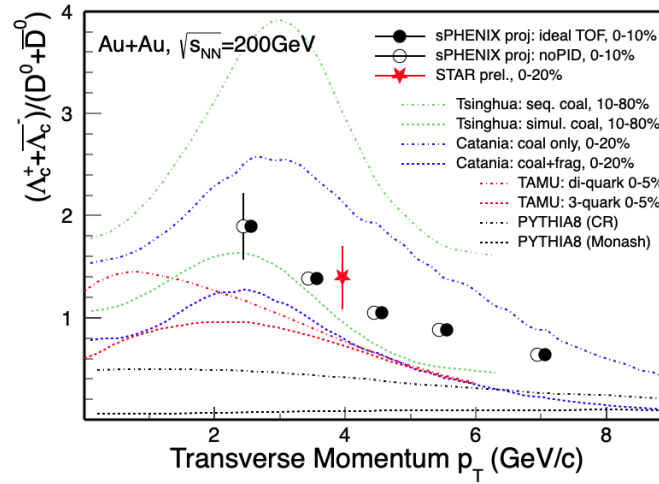


Figure 17: Physics projection plot of  $\Lambda_c/D^0$  at 0-10% as well as comparison with model calculations.

momentum/DCA resolution,  $\Lambda_c$  can be measured precisely by sPHENIX in Au+Au 200 GeV. A PID detector, such as TOF, will be very helpful for low  $p_T$   $\Lambda_c$  measurement in most central collision.

## References

- [1] X. Chen, G. Xie, and X. Dong.  $D^0$ -meson and  $B^+$ -meson production in Au+Au Collisions at  $\sqrt{s_{NN}} = 200$  GeV for sPHENIX. *sPHENIX simulation note*, sPH-HF-2017-002.
- [2] The STAR collaboration. Identified Baryon and Meson Distributions at Large Transverse Momenta from Au + Au Collisions at  $\sqrt{s_{NN}} = 200$  GeV. *Phys. Rev. Lett.*, 97(15):152301, 2006.
- [3] The STAR collaboration. Systematic measurements of identified particle spectra in pp, d + Au, and Au + Au collisions at the STAR detector. *Phys. Rev. C*, 79(3):034909, 2009.
- [4] The STAR collaboration. Strangeness enhancement in Cu + Cu and Au + Au collisions at  $\sqrt{s_{NN}} = 200$  GeV. *Phys. Rev. Lett.*, 108(7):072301, 2012.
- [5] The STAR collaboration. Centrality and transverse momentum dependence of  $D^0$ -meson production at mid-rapidity in Au + Au collisions at  $\sqrt{s_{NN}} = 200$  GeV. *Phys. Rev. C*, 99:034908, Mar 2019.
- [6] Sooraj Radhakrishnan. Measurements of open charm production in Au+Au collisions at  $\sqrt{s_{NN}} = 200$  GeV with the STAR experiment at RHIC. *Nucl. Phys. A*, 982:659–662, 2019.
- [7] The ALICE collaboration.  $\Lambda_c^+$  production in pp collisions at  $\sqrt{s_{NN}} = 7$  TeV and in p-Pb collisions at  $\sqrt{s_{NN}} = 5.02$  TeV. *J. High Energy. Phys.*, 2018(4):108, Apr 2018.

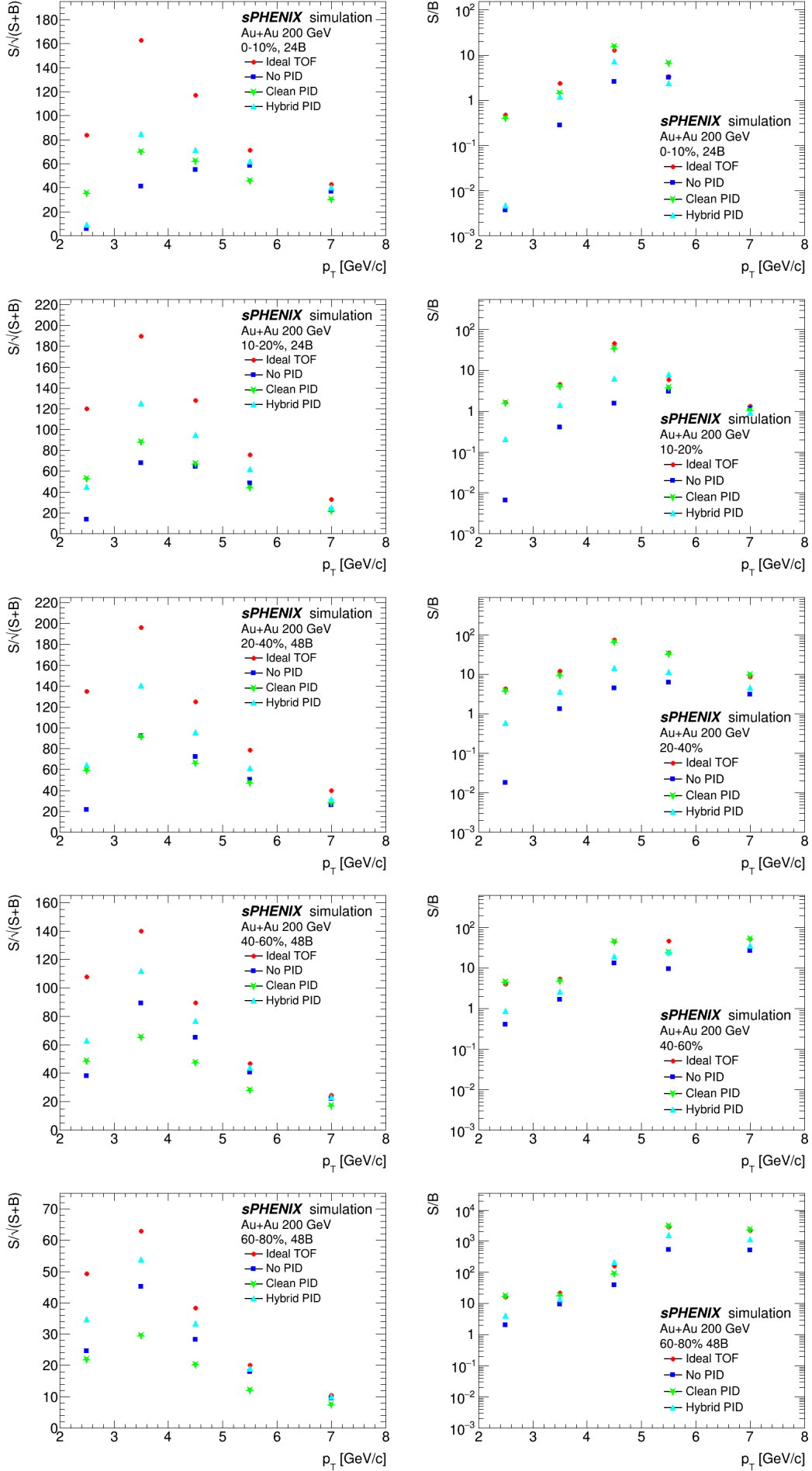


Figure 18: Significance (left) and signal to background ratio (right) under different centralities with 4 PID scenarios